THE SECOND-ORDER WAVELET SYNCHROSQUEEZING TRANSFORM

T. Oberlin [*], *S. Meignen* [†],

[*] INP–ENSEEIHT and IRIT, University of Toulouse, France
[†] Laboratoire Jean Kuntzmann, University of Grenoble, France

ABSTRACT

The paper deals with the problem of representing non-stationary signals jointly in time and frequency. We use the framework of reassignment methods, that achieve sharp and compact representations. More precisely, we introduce an enhanced version of the synchrosqueezed wavelet transform, which is shown to be more general than the standard synchrosqueezing, while remaining invertible. Numerical experiments measure the improvement brought about by using our new technique on synthetic data, while an analysis of the gravitational wave signal recently observed through the LIGO interferometer applies the method on a real dataset.

***Index Terms*—** synchrosqueezing; continuous wavelet transform; multicomponent signals; time-frequency; AM/FM; chirp detection; gravitational waves

1. INTRODUCTION

For decades, time-frequency (TF) analysis has aimed at designing new techniques for analyzing non-stationary signals, i.e. whose frequency varies across time. For instance, the Short-Time Fourier Transform (STFT), the Continuous Wavelet Transform (CWT) or the Wigner-Ville distribution [1, 2, 3] have been intensively used, for instance, in music or speech analysis, geophysics, or electrical engineering.

STFT and CWT, being the simplest of linear TF representations, are also the most popular. However, they suffer from a fundamental limitation: the Heisenberg-Gabor uncertainty principle, which limits their TF resolution. To overcome this and improve their ability to represent non-stationary signals, a pioneer work proposed in the seventies a post-processing technique to sharpen TF representations [4], which was then extended in [5] and there named *reassignment* (RM). A very similar approach followed in [6, 7] and is known as *synchrosqueezing* (SST).

The nice theoretical results stated in [7] gave a new impulse to the field, and many new developments around SST or RM have been carried out, over these last years; we can mention the use of redundancy via multitaper approaches [8, 9] or wavelet packets [10], the generalization to images [11, 12], and the application to non-harmonic waves [10]. This led to new interesting applications as, for instance, in bio-medical engineering [13] or art investigation [14].

Yet, while both SST and RM are similar techniques, their aim is quite different. The SST provides an invertible representation similar to STFT or CWT, sharp for any superposition of modulated waves, as soon as the modulation remains negligible [7]. Instead, RM provides only a sharpened TF representation, even for large frequency modulation [15], but not a reconstruction procedure. To generalize SST to non-negligible frequency modulations, the authors of this paper recently proposed to improve the definition of the instantaneous frequency (IF) estimate in the STFT setting [16]. The resulting transformation, called second-order SST (SST2), was deeply analyzed in [17]. The aim of this present paper is to extend SST2 to the CWT setting, and show, empirically, the interest of this new transformation. To this end, we first state some notation and definitions in Section 2, before introducing our new SST in Section 3. The numerical experiments presented in Section 4 show the interest of the new transformation on synthetic and real data.

2. DEFINITIONS

2.1. Continuous wavelet transform

We denote by $L^1(\mathbb{R})$ and $L^2(\mathbb{R})$ the space of integrable, and square integrable functions. Consider a signal $f \in L^1(\mathbb{R})$, and a window g in the Schwartz class, $\mathcal{S}(\mathbb{R})$, the space of smooth functions with fast decaying derivatives of any order; its Fourier transform is defined by:

$$\widehat{f}(\xi) = \mathcal{F}\{f\}(\xi) = \int_{\mathbb{R}} f(\tau) e^{-2i\pi\xi\tau} d\tau. \tag{1}$$

Let us consider an admissible wavelet $\psi \in L^2(\mathbb{R})$, satisfying $0 < C_\psi = \int_0^\infty |\widehat{\psi}(\xi)|^2 \frac{d\xi}{\xi} < \infty$. For any time t and scale $a > 0$, the *continuous wavelet transform* (CWT) of f is defined by:

$$W_f^\psi(a,t) = \frac{1}{a} \int_{\mathbb{R}} f(\tau) \psi\left(\frac{\tau - t}{a}\right)^* d\tau, \tag{2}$$

where z^* denotes the complex conjugate of z. We further assume that ψ is analytic, i.e. $\mathrm{Supp}(\widehat{\psi}) \subset [0, \infty[$, and that

The authors acknowledge the support of the French Agence Nationale de la Recherche (ANR) under reference ANR-13-BS03-0002-01 (ASTRES).

$\sup_\xi |\hat{\psi}(\xi)| = 1$. If f real-valued, CWT admits the following synthesis formula (Morlet formula):

$$f(t) = 2\mathcal{R}\left\{ \frac{1}{C'_\psi} \int_0^\infty W_f^\psi(a,t) \frac{da}{a} \right\}, \tag{3}$$

where $\mathcal{R}$ denotes the real part of a complex number and $C'_\psi = \int_0^\infty \widehat{\psi^*}(\xi) \frac{d\xi}{\xi}$.

2.2. Multicomponent signal

In this present paper, we analyze so-called *multicomponent signals* of the form,

$$f(t) = \sum_{k=1}^{K} f_k(t), \text{ with } f_k(t) = A_k(t) e^{2i\pi\phi_k(t)}, \tag{4}$$

for some K, where $A_k(t)$ and $\phi_k(t)$ are functions satisfying $A_k(t) > 0$, $\phi'_k(t) > 0$ and $\phi'_{k+1}(t) > \phi'_k(t)$ for any t and k. In the following, $\phi'_k(t)$ is often called instantaneous frequency (IF) of mode k and $A_k(t)$ its instantaneous amplitude (IA). One of the goal of TF analysis is to recover the instantaneous frequencies $\{\phi'_k(t)\}_{1\le k\le K}$ and amplitudes $\{A_k(t)\}_{1\le k\le K}$, from a given signal f. Note that with the analytic wavelets, considering complex modes or their real part $f_k(t) = A_k(t)\cos(2\pi\phi_k(t))$ is equivalent, as soon as $\phi'_1(t)$ is large enough. The CWT of a multicomponent signal is known to exhibit a ridge structure: the information is concentrated around ridges defined by $a\phi'_k(t) = 1$.

2.3. Reassignment and Synchrosqueezing

A powerful post-processing technique was introduced in [5] to sharpen the scalogram, termed reassignment method (RM). It needs the so-called reassignment operators, defined wherever $W_f(a,t) \neq 0$ by $(\hat{\omega}_f, \hat{\tau}_f) = (\mathcal{R}(\tilde{\omega}_f), \mathcal{R}(\tilde{\tau}_f))$ with

$$\begin{cases} \tilde{\omega}_f(a,t) = \dfrac{1}{2i\pi} \dfrac{\partial_t W_f(a,t)}{W_f(a,t)} \\ \tilde{\tau}_f(a,t) = \dfrac{\int_{\mathbb{R}} \tau f(\tau) \frac{1}{a}\psi\left(\frac{\tau-t}{a}\right)^* d\tau}{W_f(a,t)}. \end{cases} \tag{5}$$

These operators locally define an IF and a group delay (GD), and they estimate the position of a ridge if it is close enough. Then, RM consists in moving the coefficients of the scalogram according to the map $(a,t) \mapsto (\hat{\omega}_f(a,t), \hat{\tau}_f(a,t))$. We know, from [5], that RM perfectly localizes linear chirps with constant amplitude. Alternatively, SST reassigns the coefficients of the CWT in the time-scale plane according to the map $(a,t) \mapsto (\hat{\omega}_f(a,t), t)$ [7]:

$$T_f(a,t) = 2\mathcal{R}\left\{ \frac{1}{C'_\psi} \int_{\{b, |W_f^\psi(b,t)| \ge \gamma\}} W_f^\psi(b,t) \delta(\hat{\omega}_f(a,t) - b) \frac{db}{b} \right\}, \tag{6}$$

and then reconstruction of f_k is performed through:

$$f_k(t) = \int_{|1 - a\phi'_k(t)| < d} T_f(a,t) da. \tag{7}$$

Since the (complex) coefficients are moved only along the scale axis, the transform remains invertible using formula (3). But, since GD is ignored, the method cannot handle large frequency modulations: the perfect localization property is only ensured for purely harmonic waves [6, 7].

3. SECOND-ORDER SYNCHROSQUEEZING

On one hand, RM provides a nice representation for a wide range of AM/FM or multicomponent waves. On the other hand, SST is invertible, but only suitable for low-modulated waves ($|\phi''(t)| \ll \phi'(t)$). SST2, introduced in [16] in the STFT context, aims to combine both properties, by improving IF estimate $\hat{\omega}_f$.

3.1. An improved instantaneous frequency

To start with, we locally estimate the frequency modulation $\phi''(t)$, by means of the following operator:

$$\tilde{q}_f(a,t) = \frac{\partial_t \tilde{\omega}_f(a,t)}{\partial_\tau \tilde{t}_f(a,t)}, \tag{8}$$

which enables us to define a new complex estimate:

$$\tilde{\omega}_f^{(2)}(a,t) = \begin{cases} \tilde{\omega}_f(a,t) + \tilde{q}_f(a,t)(t - \tilde{\tau}_f(a,t)) & \text{if } \partial_t \tilde{t}_f(a,t) \neq 0 \\ \tilde{\omega}_f(a,t) & \text{otherwise,} \end{cases} \tag{9}$$

and then $\hat{\omega}_f^{(2)}(a,t) = \mathcal{R}(\tilde{\omega}_f^{(2)}(a,t))$, as a new IF estimate. The new synchrosqueezing operator is then defined by replacing $\hat{\omega}_f$ by $\hat{\omega}_f^{(2)}$ in (6). Note that the definition is very similar in the STFT context [16].

3.2. Computation

CWT is computed scale by scale in the Fourier domain, thanks to the Plancherel theorem:

$$W_f^{\hat{\psi}}(a,t) := W_f^\psi(a,t) = \int_{\mathbb{R}} \hat{f}(\xi)\hat{\psi}(a\xi)^* e^{2i\pi t\xi} \, d\xi. \tag{10}$$

We denote by $W_f^{\hat{\psi}}$, $W_f^{\xi\hat{\psi}}$ and $W_f^{\hat{\psi}'}$ the CWTs corresponding, in the Fourier domain, to wavelets $\hat{\psi}$, $\xi\hat{\psi}$ and $(\hat{\psi})'$. We easily get:

$$\begin{aligned} \partial_t W_f^{\hat{\psi}}(a,t) &= \frac{2i\pi}{a} W_f^{\xi\hat{\psi}}(a,t) \\ \tilde{\tau}_f(a,t) W_f^{\hat{\psi}}(a,t) &= t W_f^{\hat{\psi}}(a,t) + \frac{a}{2i\pi} W_f^{\hat{\psi}'}(a,t). \end{aligned} \tag{11}$$

Then, the reassignment operators (5) can be written:

$$\begin{cases} \tilde{\omega}_f(a,t) = \dfrac{W_f^{\xi\hat{\psi}}(a,t)}{aW_f^{\hat{\psi}}(a,t)} \\ \tilde{\tau}_f(a,t) = t + \dfrac{a}{2i\pi}\dfrac{W_f^{\hat{\psi}'}(a,t)}{W_f^{\hat{\psi}}(a,t)}. \end{cases} \tag{12}$$

By differentiating and using equation (11) again, we finally obtained

$$\tilde{q} = \frac{2i\pi}{a^2}\frac{W^{\xi^2\hat{\psi}}W_f^{\hat{\psi}} - (W_f^{\xi\hat{\psi}})^2}{W_f^{\hat{\psi}} + W_f^{\xi\hat{\psi}'}W_f^{\hat{\psi}} - W_f^{\hat{\psi}'}W_f^{\xi\hat{\psi}}}, \tag{13}$$

where $W_f^{\xi\hat{\psi}'}$ and $W_f^{\xi^2\hat{\psi}}$ denote the CWTs computed using the wavelets $\xi \mapsto \xi(\hat{\psi})'$ and $\xi \mapsto \xi^2\hat{\psi}$, the variables (a,t) being omitted to lighten the notation.

3.3. A second-order SST

We term our new SST "second-order", because it manages to perfectly localize linear chirps:

Theorem 3.1. *Let $h(t) = A(t)e^{2i\pi\phi(t)}$, with $A(t) = Ae^{-P(t)}$, where $A > 0$, $P(t) > 0$ and P and ϕ are second-order polynomials. Then we have, wherever $W_h(a,t) \neq 0$,*

$$\hat{\omega}_f^{(2)}(a,t) = \phi'(t). \tag{14}$$

Proof. We have the following expansion for any $t, \tau \in \mathbb{R}$:

$$h(\tau) = h(t)e^{(2i\pi\phi'(t) - P'(t))(\tau - t) + (i\pi\phi''(t) - \frac{P''(t)}{2})(\tau - t)^2}. \tag{15}$$

Then, we can write

$$W_h(a,t) = \frac{h(t)}{a}\int_{\mathbb{R}} e^{(i\pi\phi''(t) - \frac{P''(t)}{2})\tau^2}\psi\left(\frac{\tau}{a}\right)^* e^{(2i\pi\phi'(t) - P'(t))\tau}\, d\tau$$

$$\partial_t W_h(a,t) = \left[2i\pi\phi'(t) - P'(t)\right] W_h(a,t) + \left[2i\pi\phi''(t) - P''(t)\right] W_h(a,t)(\tilde{\tau}_f(a,t) - t).$$

We finally get

$$\tilde{\omega}_f(a,t) = \left[\phi'(t) - \frac{P'(t)}{2i\pi}\right] + \left[\phi''(t) - \frac{P''(t)}{2i\pi}\right](\tilde{\tau}_f(a,t) - t).$$

Differenting each side with respect to t, we immediately get: $\tilde{q}_f(a,t) = \phi''(t) - \frac{P''(t)}{2i\pi}$, from which we deduce,

$$\phi'(t) = \mathcal{R}\left(\tilde{\omega}_f(a,t) + \tilde{q}_f(a,t)(t - \tilde{\tau}_f(a,t))\right) = \hat{\omega}_f^{(2)}(a,t)$$

□

Remark: In [17], we proved a stronger result for the STFT, showing that the good localization property still holds for quasi-linear chirps, i.e. when we have $|\phi'''(t)| \ll 1$. A similar result should be available in the CWT context for modes satisfying $|\phi'''(t)| \ll \phi'(t)$, but this is left for future investigations.

4. NUMERICAL EXPERIMENTS

4.1. Representation and decomposition of a synthetic signal

We consider a synthetic 3-modes multicomponent signal, made of a pure wave, an exponential chirp and an hyperbolic chirp, whose instantaneous frequencies are respectively constant, exponential ($\phi''(t) \propto \phi'(t)$) and hyperbolic ($\phi''(t) \propto \phi'(t)^2$). CWT and SST of our test-signal are displayed in Figure 1; we can clearly see on the representation of SST the 3 ridges corresponding to the modes, but the corresponding coefficients are spread out around these ridges. This is because, except for pure harmonic waves, the frequency modulation is not negligible and should be taken into account in IF estimation.

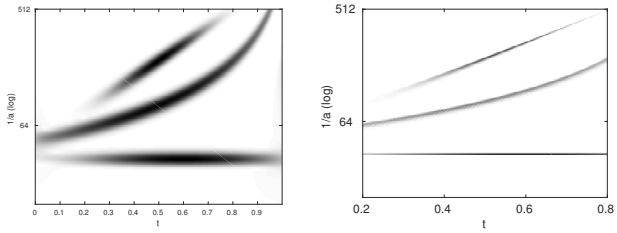

Fig. 1. CWT and SST of the synthetic signal.

Now we consider a noisy version of this test-signal (with input SNR = 10 dB), and compare, in the following Figure 2, the representations given by SST, SST2 and RM. It is clear that both SST2 and RM achieve a compact representation, although it is corrupted by a non-negligible noise. Now, if we reconstruct the different modes from the synchrosqueezed representations, we just need to sum the vertical coefficients around a ridge, as expressed in (7). If we take 3 coefficients per ridge (parameter d in (7)) and per time sample, we end up with an accuracy of 14 dB for SST, and 21 dB for our SST2.

To better assess the superiority of SST2, we now compare the obtained results with the ideal time-frequency representation, by means of the Earth Mover Distance (EMD), as done in [18]. The EMD is a sliced Wasserstein distance, commonly used in optimal transport, which allows for the comparison of two distributions. In Figure 3, we show EMD computed for the exponential chirp of Figure 1, different input SNRs and different representations (the lower the EMD, the better). We see that the reassigned representation (RM) achieves the best performance whatever the input SNR, and also that SST2 is relatively close. In contrast, the representation given by SST is quite poor. The improvement brought about by SST2 or RM is particularly significant at low noise levels, but remains whatever the input SNR.

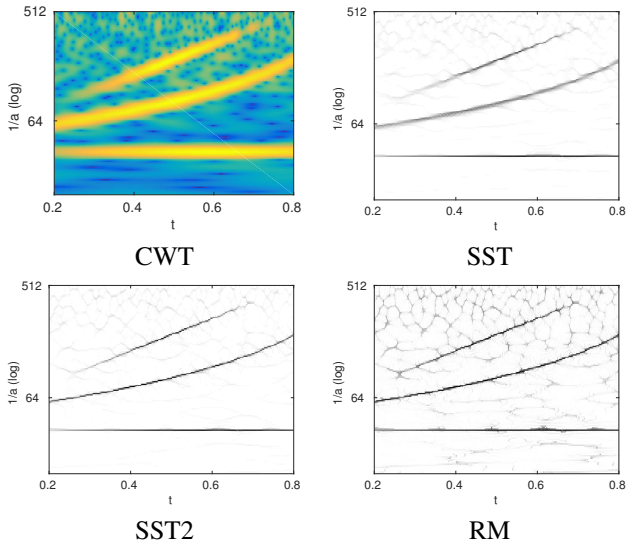

Fig. 2. Time-frequency representations of the noisy synthetic signal, with input SNR = 10 dB.

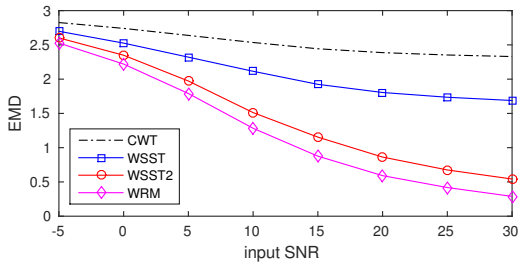

Fig. 3. EMD as a function of Input SNR, for different representations.

4.2. Application on real data

We now illustrate an application of our technique on the gravitational wave signal recorded last year [19], which had a considerable impact in the scientific community. The signal recorded by the LIGO interferometer is typically a chirp with large frequency modulation, for which the SST2 clearly improves the result. We consider the pre-processed signal from Hanford interferometer, available online at `https://losc.ligo.org/s/events/GW150914/P150914/fig1-waveform-H.txt`. We display, in Figure 4, its TF representations given by SST and SST2, obtained with the complex Morlet wavelet with $\sigma = 0.8$. Both representations show a nice ridge with increasing IF, but SST2 is more concentrated. We also show the same representations, with the estimated ridge superimposed. The results differ significantly, since only SST2 allows us to recover the complete "ringdown", which is the part of the signal emitted after the fusion of the two blackholes.

If we reconstruct the chirp using both representations, we observe that SST2 gives a result closer to the expected one that SST does: the SNR is 6.45 dB for SST and 7.81 dB for SST2. Time curves displayed in Figure 4 also show that the ringdown part of the chirp is better recovered using SST2.

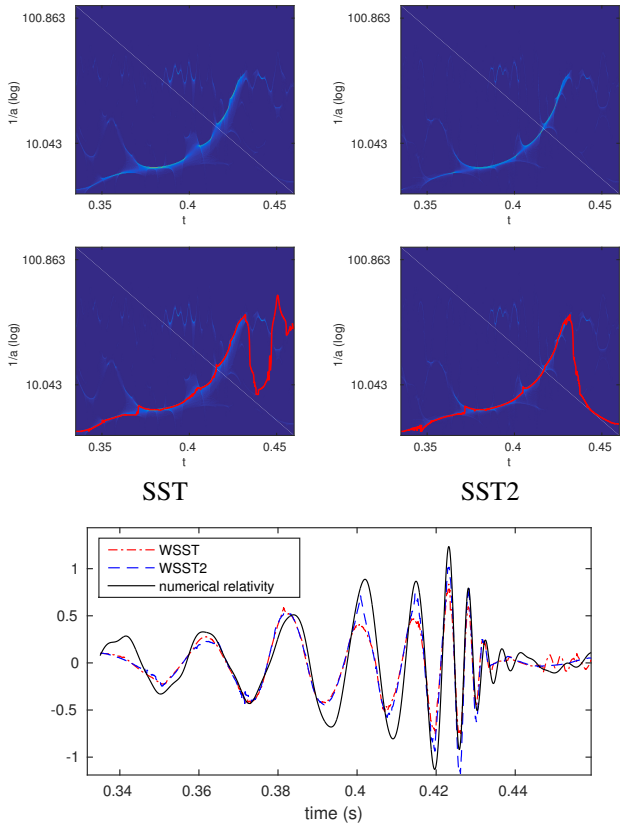

Fig. 4. From top to bottom : TF representation of the Hanford signal, the estimated ridge, and the reconstruction, for SST (left) and SST2 (right).

5. CONCLUSION

We introduced in this paper the second order SST, which is the counterpart for wavelets of the STFT-based SST2 defined in [16]. Similar to the STFT context, the new transformation was shown to perfectly localize linear chirps, and to remain efficient when the frequency modulation is quasi-linear. Numerical experiments illustrated the benefit of SST2 over standard synchrosqueezing, and recalled the main differences between STFT and CWT for analyzing multicomponent signals. Future works should build a theoretical analysis of SST2, to extend the results of [17]. On an applicative point of view, the next step would be to combine the method introduced here with other recent improvements of SST [9, 10], which should lead to significantly better performance.

6. REFERENCES

[1] P. Flandrin, *Time-frequency / Time-scale Analysis*, vol. 10, Academic press, 1998.

[2] Leon Cohen, *Time-frequency analysis*, vol. 778, Prentice hall, 1995.

[3] S. G. Mallat, *A wavelet tour of signal processing*, Academic Press, 1999.

[4] K. Kodera, C. De Villedary, and R. Gendrin, "A new method for the numerical analysis of non-stationary signals," *Physics of the Earth and Planetary Interiors*, vol. 12, no. 2, pp. 142–150, 1976.

[5] F. Auger and P. Flandrin, "Improving the readability of time-frequency and time-scale representations by the reassignment method," *IEEE Trans. Signal Process.*, vol. 43, no. 5, pp. 1068–1089, 1995.

[6] I. Daubechies and S. Maes, "A nonlinear squeezing of the continuous wavelet transform based on auditory nerve models," *Wavelets in Medicine and Biology*, pp. 527–546, 1996.

[7] I. Daubechies, J. Lu, and H.-T. Wu, "Synchrosqueezed wavelet transforms: An empirical mode decomposition-like tool," *Appl. Comput. Harmon. Anal.*, vol. 30, no. 2, pp. 243–261, 2011.

[8] J. Xiao and P. Flandrin, "Multitaper time-frequency reassignment for nonstationary spectrum estimation and chirp enhancement," *IEEE Trans. Sig. Proc.*, vol. 55, no. 6, pp. 2851–2860, 2007.

[9] I. Daubechies, Y.G. Wang, and H.-T. Wu, "ConceFT: concentration of frequency and time via multitapered synchrosqueezed transform," *Philosophical Transactions of the Royal Society of London A: Mathematical, Physical and Engineering Sciences*, vol. 2065, no. 374, 2016.

[10] H. Yang, "Synchrosqueezed wave packet transforms and diffeomorphism based spectral analysis for 1D general mode decompositions," *Applied and Computational Harmonic Analysis*, vol. 39, no. 1, pp. 33–66, 2015.

[11] H. Yang and L. Ying, "Synchrosqueezed wave packet transform for 2D mode decomposition," *SIAM Journal on Imaging Sciences*, vol. 6, no. 4, pp. 1979–2009, 2013.

[12] M. Clausel, T. Oberlin, and V. Perrier, "The monogenic synchrosqueezed wavelet transform: a tool for the decomposition/demodulation of AM-FM images," *Applied and Computational Harmonic Analysis*, vol. 39, no. 3, pp. 450 – 486, 2015.

[13] H-T. Wu, Y-H. Chan, Y-T. Lin, and Y-H. Yeh, "Using synchrosqueezing transform to discover breathing dynamics from ecg signals," *Applied and Computational Harmonic Analysis*, vol. 36, no. 2, pp. 354–359, 2014.

[14] H Yang, J Lu, W. P. Brown, I. Daubechies, and L. Ying, "Quantitative canvas weave analysis using 2-d synchrosqueezed transforms: Application of time-frequency analysis to art investigation," *IEEE Signal Processing Magazine*, vol. 32, no. 4, pp. 55–63, 2015.

[15] François Auger, Patrick Flandrin, Yu-Ting Lin, Stephen McLaughlin, Sylvain Meignen, Thomas Oberlin, and Hau-Tieng Wu, "Time-frequency reassignment and synchrosqueezing: An overview," *IEEE Signal Processing Magazine*, vol. 30, no. 6, pp. 32–41, 2013.

[16] T. Oberlin, S. Meignen, and V. Perrier, "Second-order synchrosqueezing transform or invertible reassignment? Towards ideal time-frequency representations," *Signal Processing, IEEE Transactions on*, vol. 63, no. 5, pp. 1335–1344, March 2015.

[17] R. Behera, S. Meignen, and T. Oberlin, "Theoretical analysis of the second-order synchrosqueezing transform," 2015.

[18] S. Peleg and M. Werman, "Fast and robust earth mover's distances," in *IEEE Int. Conf. Computer. Vision.*, 2009, pp. 460–467.

[19] B. P. Abbott et al., "Observation of gravitational waves from a binary black hole merger," *Physical review letters*, vol. 116, no. 6, pp. 061102, 2016.